UAV Icing: Experimental Analysis of Icing on a Rotor of a UAV

Nicolas C. Müller[1,2], Richard Hann[1,2]

[1] *Norwegian University of Science and Technology, NTNU, Trondheim, Norway*
[2] *UBIQ Aerospace AS, Trondheim, Norway*

nicolas.c.muller@ntnu.no, richard.hann@ntnu.no

Abstract— **Rotors are the most sensitive part of small multi-rotor uncrewed aerial vehicles (UAVs) to atmospheric in-flight icing. Ice accumulation on a rotor can reduce the ability of the rotor to produce lift and thrust and increase the required propulsion power. If the required propulsion power exceeds the capabilities of the powertrain, the UAV might lose its ability to maintain its altitude and stability, which can have catastrophic consequences. In this study, the performance of a UAV rotor is analysed in horizontal flight and vertical climb in icing conditions. An icing wind tunnel was used to test a 381 mm UAV rotor in icing conditions at two temperatures of −5 °C and −10 °C. The impact of icing on the propeller is examined by measuring and analysing the rotor's change in thrust and torque. A high-speed camera is used to record and observe the dynamic ice accretion, and a photogrammetry-based method is used to extract the ice shape at the end of the ice accretion process. This study reveals that the propeller responds differently to ice accretion in thrust and lift configurations. In the vertical lift configuration, the rotor's lift stayed constant in icing after an initial drop of 20%, while in the horizontal rotor configuration, the rotor's thrust declined continuously during the ice accretion process. The rotor's torque has increased linearly with the ice accretion time in both configurations. This is done to assess the influence of icing on the rotor of a multi-rotor UAV, to understand the risk of icing for a UAV. This data can be used to detect the existence of ice on the UAV based on its rotors, and to evaluate mitigation methods for icing on UAV rotors.**

Keywords— ***UAV, Propeller, Inflight-Icing, Rotor, Atmospheric Icing, Wind tunnel***

I. INTRODUCTION

The capabilities of uncrewed aerial vehicles (UAVs), also called remotely piloted vehicles (RPAS) or unmanned aerial systems (UAS) have developed a lot in the last few years, which has led to an increased use of UAVs in commercial and military applications [1,2]. With these increased applications, the operational availability of UAV services becomes more critical. One significant limitation to the use of UAVs is adverse weather. One especially critical adverse weather condition is atmospheric in-flight icing. [3] This describes the condition, in which liquid water exists in clouds at temperatures below the freezing point. When flying through those conditions, the droplets can freeze upon contact with the aircraft, leading to ice accumulations [3].

This ice accumulation can have severe implications on the aerodynamic performance of UAVs by increasing the drag and the weight of the UAV while at the same time reducing the maximum lift [4]. This can lead to the loss of control of the UAV. The ice accretion is especially critical for UAVs, as the ice accumulation is faster at the lower Reynolds numbers common with UAVs [5,6].

One part of a UAV that is especially sensitive to icing are the propellers or rotors of the UAV[7]. This sensitivity is due to their higher velocity through the air, and the smaller chord length, which enables a significantly faster ice accumulation compared to wing. This ice accumulation can lead to the loss of thrust within a minute [8]. For multi-rotor UAVs, this loss of thrust additionally leads to a loss of control since the thrust generated by the rotors is directly used to lift the UAV and control the UAV [9].

The flow conditions around the rotor of a multi-rotor UAV are dependent on the current flight state. Three different flight conditions for rotary wing aircraft can be identified: hover, stationary climb, and forward flight [10]. In hover, the forward flight velocity of the aircraft is zero, in which case, the flow of the air through the rotors is only the induced airflow generated by the rotors to create lift. In a stationary climb, an additional velocity component is created by the climbing speed of the UAV. This increases the airflow through the rotor. If the UAV is in forward flight, the airflow through the rotor has a component perpendicular to the rotation axis. This flow component leads to flow conditions, which change during the rotation of the rotor dependent on the position of the rotor blade relative to the direction of the flight of the UAV [11, 12].

The young field of icing on UAVs has initially focussed on icing analysing the ice accretion on the wings of UAVs[6]. It was observed that a reduction in the Reynolds number leads to an increase in the water collection efficiency on the wings, which increases the performance degradation of wings in icing conditions if the sizes of the test object decrease [13].

Experiments on the propellers of UAVs have shown that ice accretion on the propeller can lead to a very rapid decrease in its performance, especially in glaze icing conditions, which occur at high temperatures and are classified by complex ice shapes [14].

Research has shown that the degree of performance loss of UAV propellers in icing conditions strongly depends on the ice shedding. Ice shedding occurs when the ice breaks of the propeller due to centrifugal forces, which leads to a recovery of the performance. Ice shedding occurs after longer ice accretion at colder temperatures. and thus, the performance degradation on UAV propellers is more substantial at lower temperatures, as ice shedding occurs later and is more violent at those temperatures [15].

The performance degradation of the propeller is dependent on the liquid water content (LWC) and the mean volume diameter (MVD) of the droplets in the air. Both factors affect the ice thickness and the ice shapes.[16].

This paper aims to analyse the influence of the flight direction of the multi-rotor UAV on the ice accretion on the rotor. To evaluate the difference in the performance of the

rotor, the ice accretion on the rotor is tested both in horizontal flight conditions, in which the rotation axis is perpendicular to the airflow and in a vertical climb configuration, in which the rotation axis is aligned with the rotation of the rotor.

This work helps to define the influence of icing on small multi-rotor UAVs in different flight conditions. Understanding the ice accretion is important to evaluate the behaviour of UAV rotors in icing conditions and develop numerical methods to predict the ice accretion on the rotors of UAVs. Understanding the ice accretion on UAV rotors is a key step to developing UAVs that can operate in icing conditions, and expand the use of UAVs in cold climates.

II. Methods

A. Icing wind tunnel

The experiments were performed at the VTT icing wind tunnel in Helsinki [17]. The tunnel can deliver wind speeds up to 50 m/s and temperatures down to −25 °C.

A Flight Stand 1580 dynamometer was used to measure thrust and lift of the propeller [18]. The force measurement unit was placed in the centre of the test section. It was mounted in two different orientations, as can be seen in Fig. 1. The orientations were used to emulate the conditions experienced in different flight situations of a multirotor UAV. The thrust position, with the rotation axis aligned with the flow is representative of a vertical climb of the UAV, and the lift configuration with the rotation axis perpendicular to the flow represents the horizontal flight of the UAV.

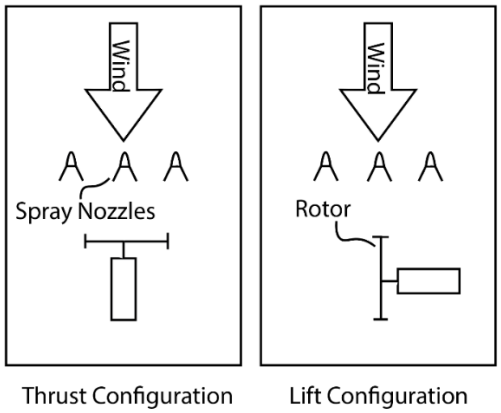

Fig. 1 The propeller test setup in the wind tunnel in the lift configuration.

A Phantom Veo710L high-speed camera was used to record phase-locked images of the rotor during the ice accretion process [19]. The camera was synchronised by a laser beam that was triggered by the rotating rotor blades passing through the beam. An Arduino Uno digitised this signal and to trigger the high-speed camera and 4 MultiLED QT lights that were used as illumination, which are also controlled by the Arduino.

The test was performed with constant rotation rate and constant thrust modes. Testing with a constant rotation rate enables easier comparison of the experiments with numerical simulations, while a constant thrust experiments are more consistent with real fighting conditions. Both modes were controlled by a custom JavaScript code running inside the RC-Benchmark software that controls the test stand.

After the experiment, for selected icing runs, a 3D scan of the ice shape was performed using photogrammetry based on the process indicated in [20]. For this, the propeller was removed from the test stand in the icing wind tunnel. The ice mass on the propeller was measured, after which the propeller was painted with white acrylic paint. The rotor was placed in a freezer at −20 °C for the paint to freeze. The propeller was now placed on a turntable, and 48 evenly spaced pictures were taken of the propeller with a Sony A6400 camera using a SEL5018 Lens. The images were loaded into the photogrammetry software Agisoft Metashape, and a 3D geometry was created. This 3D geometry was then analysed using Tecplot to extract the cross sections of the ice shape. Cross sections were extracted at 75% of the radius of the rotor to compare the results of different rotor tests.

B. Test Conditions

The experiment was performed at two different temperatures, −5 °C and −10 °C. In total 25 test runs were performed in horizontal and vertical configuration. Further variations were the used rotation rate and the LWC. Two LWCs were used, one at 0.6 g/m^3 and one at 1.8 g/m^3. The LWC was calibrated at the end of the wind tunnel at 25 m/s airspeed using a round cylinder [21]. The LWC was corrected by correlating the airspeed used for the calibration and the airspeed used for testing.

TABLE I. Test Conditions

Element	Range	Unit
Temperature	−5, −10	°C
MVD	22.7	µm
LWC	0.56, 1.80	g/m^3
Velocity	6	m/s
Rotation Rate	4400-5000	rpm
Duration	120-240	s
Lift	10	N

C. Test objects.

The experiments were performed on a 15x5 rotor manufactured and sold by Mejzlik Propellers sro. [22]. The diameter of the rotor is 15 inches or 381 mm. The rotor is a representative rotor size for multirotor UAVs with a weight of about 3-5 kg.

III. Results

Figure 2 shows the results of the tests performed at −5 °C. Three different test results are plotted. A constant rotation rate test at 5000 rpm in thrust and lift configuration, as well as a constant rotation test at 4400 rpm test in lift configuration. For both tests in lift configuration, the recorded thrust shows a slight decline from 11 N to 9 N, after which the measured thrust stays stable. The experiment in thrust configuration shows the same initial thrust decline, followed by a gradual reduction in thrust, which continues until the test stopped after 90 s. The recorded torque during all the experiments is increasing linearly during the initial ice accretion phase. The gradient of the torque increase is similar for both the 5000 rpm runs and lower for the 4400 rpm experiment. The test at 5000 rpm in thrust configuration was stopped after 80 s

because the current drawn by the motor exceeded the rating of the speed controller.

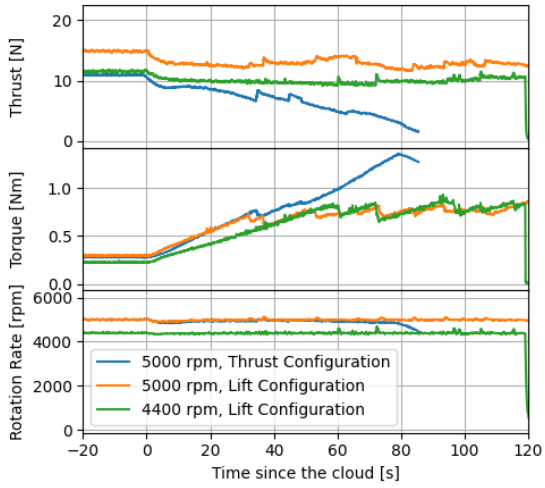

Fig. 2 Thrust and torque development for the experiment at 1.5 g/m³ at −5 °C.

In Fig. 3, the thrust and torque development for the experiments performed at −10 °C are shown. Here, a constant rotation test in lift configuration is performed at 4400 rpm and in thrust configuration at 5000 rpm. A constant thrust test at 10 N of thrust in lift configuration is also shown.

Both the constant thrust run and the constant rotation rate run in the lift condition experiment show a constant thrust of 10 N during the experiment. The thrust configuration test shows a gradual decline in thrust, which is then followed by a sudden increase in thrust and subsequent decrease. The sudden thrust increases correlate to a visual loss of ice on the rotor (ice shedding), observed from high-speed camera footage. The constant thrust case shows a variation in the rotation rate, which correlates with the chances in the torque. The efficiency of the rotor in the thrust case decreased by 300%.

The torque increased at similar gradients for all the experiments, and after 50 seconds, all experiments showed frequent sudden reductions in the torque, again aligned with changes in thrust at the same time and loss of ice on the high-speed camera. This is again explained by ice shedding.

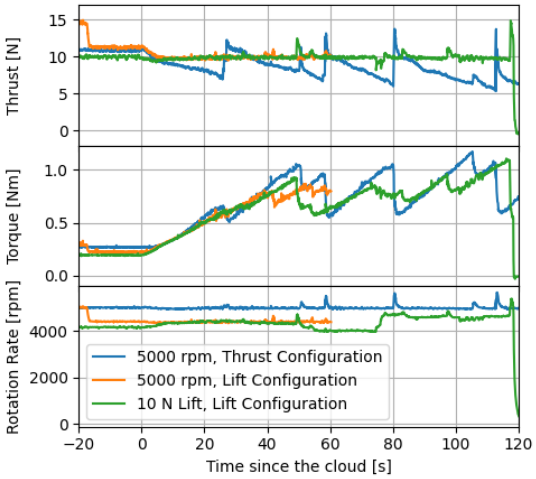

Fig. 3 Thrust and torque development for the experiment at 1.5 g/m³ at −10 °C.

In Fig. 4, the ice on the propeller is shown before and after the ice-shedding event after 58 seconds of ice accretion in the 5000 rpm thrust configuration case. A large portion of the ice on the rotor is missing from the after picture.

a)

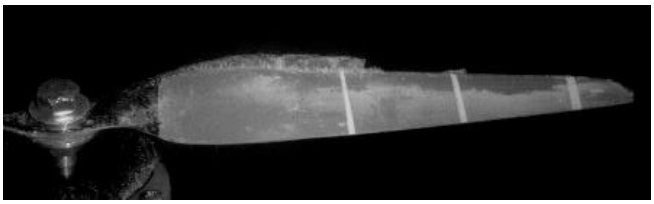

b)

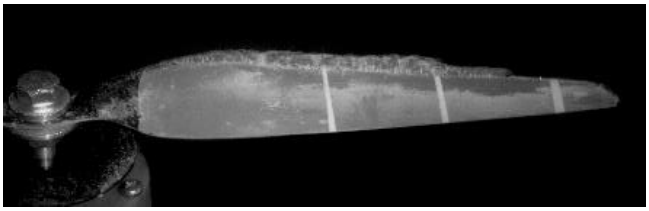

Fig. 4 Ice on the propeller a) before and b) after an ice shedding event with a LWC of 1.5 g/m³ at −10 °C with a rotation rate of 5000 rpm and in thrust configuration.

The change in the performance of the rotor in thrust configuration for different LWCs can be seen in Fig. 5. Here, it is shown that the gradient of the performance degradation decreases with a reduced LWC. The reduction in thrust occurs at a similar gradient compared to the higher LWC, while the increase in torque of the rotor happens at a lower rate at the lower LWC. The observed ice-shedding events are also not as significant as the ice-shedding events observed at the higher LWC. The thrust and torque values reached before the ice shedding events start are similar to those values measured with the higher LWC. This behaviour leads to a lower mean thrust value and a higher torque value.

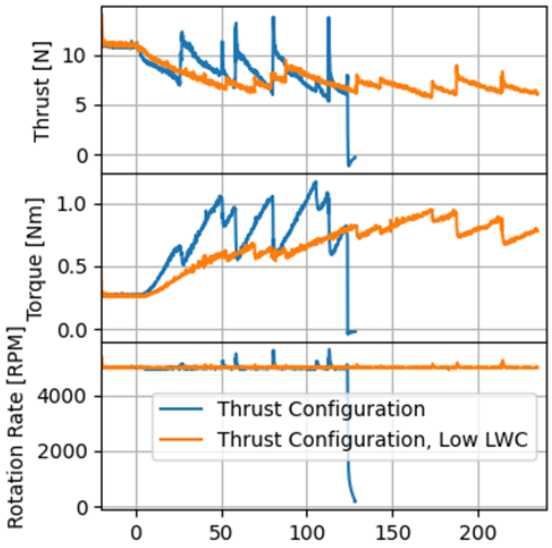

Fig. 5 Thrust and torque development for the experiment at 1.5 g/m³ at −5 °C.

In Fig. 6, the first ice shedding event on a blade for the experiments shown in Fig. 5 after 30 s for the high LWC and 60 s at the low LWC. At the higher LWC, more ice has accumulated on the propeller prior to the ice-shedding event. The ice shape that has formed is more complex, with a development of feathers and lobster tails, while at the low LWC, the ice shape does show less variance.

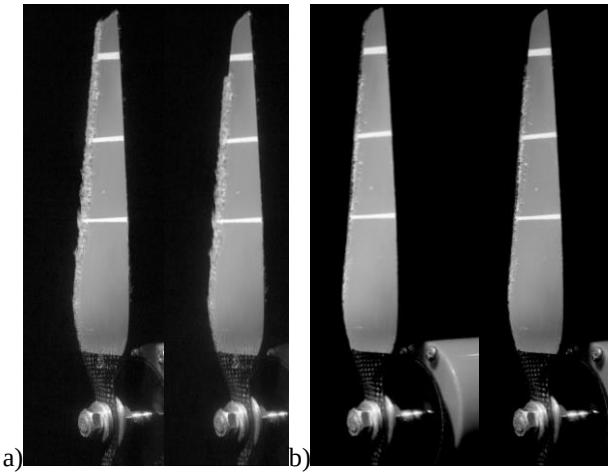

Fig. 6 First Ice shedding on a blade for the experiment at 1.5 g/m³ at -5 °C in thrust configuration at a) high or b) low LWC. One picture is before, and one after the ice-shedding.

The dependency of the performance degradation on the thrust and torque values for the lift configuration is shown in Fig. 7. This plot shows the thrust and torque values for an experiment performed at 4400 rpm. A third line is displayed, which shows the measured thrust and torque for the low LWC, where the time axis is reduced by the difference in the LWC, thus indicating the performance relative to the total amount of water collected by the rotor. This line is very close to the performance degradation by the high LWC, indicating that the performance degradation of the rotor is most strongly associated with the total amount of water collected.

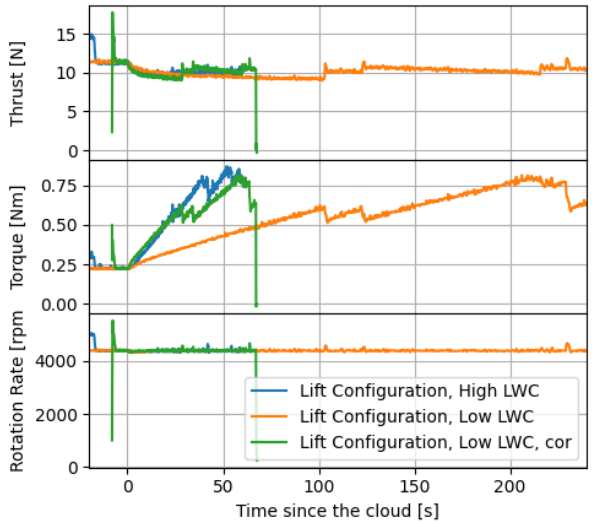

Fig. 7 Performance degradation in lift configuration at -10 °C, with a LWC of 0.56 g/m³ and 1.8 g/m.³.

In Fig. 8, the ice shapes, as captured by the photogrammetry method, are shown for the lift configuration at 4400 rpm. Tyhe ice shape at −5 °C is significantly more complex than at −10 °C. It displays multiple small features that change in chordwise and radial directions. The ice shape at −10 °C is more uniform and displays only a slight radial variation, a few small scale features. The difference in the ice shapes can also be seen on the cross-section taken at 75% of the radius. The ice shape at −5 °C has more minor variations resembling horns, representing the small radiuswise features. The ice shape at -10 °C is a more uniform ice block. Additionally, the icing extend is smaller at −10 °C on the top and bottom surfaces.

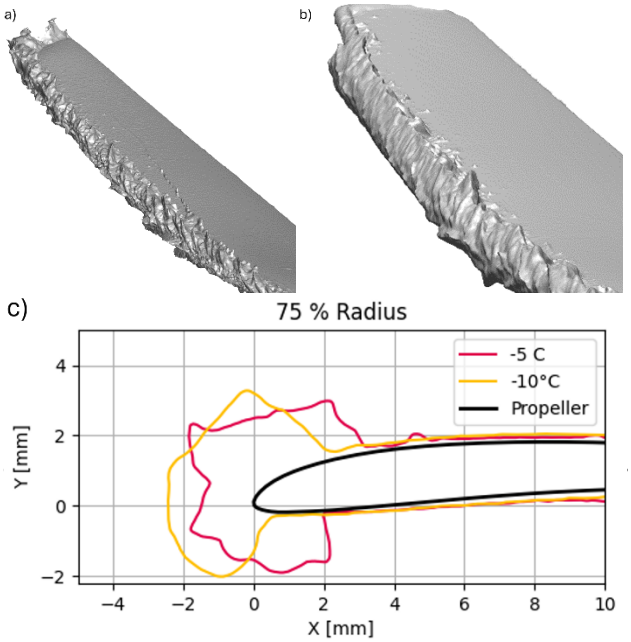

Fig. 8 Ice shapes at 4400 rpm and in lift configuration after 60 s of ice accretion at the low LWC a) at −5 °C, b) at −10 °C, and c) a cross section.

IV. Discussion

One of the considerable challenges of testing the performance of rotors in an IWT is the possible blockage of the wind tunnel by the rotor. In this experiment, diameter of the rotor is 54% of the width of the testing section, which means that the performance of the rotor affected by the rotor, compared to the free stream. The restricted test section size will affect both configurations, where the lift configuration is likely more affected [23].

The work aimed to test the rotor in comparable conditions, both in thrust and lift configurations. Therefore, the rotation rate was fixed to achieve 10 N of thrust in both configurations. This increase in the rotation rate for the thrust configuration seems to have increased the ice accretion rate on the rotor, which leads to a larger performance degradation. This is especially visible in the change in the torque of the rotor.

The icing has only a very limited influence on the thrust of the rotors in lift configuration. This effect could be caused by multiple reasons, one being the difference in the local angle of attack of the rotor blades relative to the inflow, which leads to different impingement pattern and thus ice shapes. Especially the large ice accretion on the trailing edge could increase the lift the rotor is generating on the cost of increased drag. The

difference could also be due to the reduced ice accretion on the lift configuration rotor close to the tip. If less ice is accumulated on the tip, this could reduce the impact the icing has on the thrust generated by the rotor. This behaviour is consistent with findings in other research [9,10], but it could be caused by the proximity of the walls of the wind tunnel. The proximity of the walls could influence the flow patterns around the rotor, especially by redirecting the wake of the rotor to remain inside the wind tunnel confinement. This could increase the measured lift compared to a free stream situation. Further research needs to be done, to evaluate if the reason for this behaviour is due to the ice accumulation, or caused by the experimental setup.

A second observation of the experiments is that the speed of the performance degradation is proportional to the LWC at −10 °C. This is significant for the developments of models for the behaviour of UAV rotors in icing conditions. This is likely caused by a very high freezing fraction on the rotor, even at the high LWC condition, and thus might not be accurate for very high LWCs or high temperatures.

The rotor in the thrust condition at −5 °C has less severe ice-shedding events at low LWC compared to the high LWC. They occur earlier in the ice accretion process, but once the ice shedding has led to a steady performance level , the performance degradation is similar to the high LWC. The difference could be caused by a change from a glaze ice to a mixed ice condition. A different ice regime could lead to an ice with less cohesion, and the voids in the ice shape would enable the more frequent shedding of small ice blocks. This would be caused by the increase in ice adhesion at lower temperatures with a simultaneous decrease in cohesion. This hypothesis is supported by the ice shapes observed in the high-speed camera images during the ice accretion process, which show different ice morphologies at the first ice shedding.

V. Conclusions

Icing on the rotors of UAVs is a significant issue that must be addressed to operate them safely in icing conditions. The influence of the ice accumulation on the aerodynamic performance is such that the power required to run the propeller may increase by more than 300%. Thus, a safe flight of the UAV is not be guaranteed if a UAV enters icing conditions. The experiments have shown a significant difference between the performance degradation seen in a lift or a thrust configuration, where in a lift condition the thrust generated by the rotor stays rather constant. In a thrust configuration the thrust of the rotor will decrease during the ice accretion. Significant areas of research for future evaluation are the ice-shedding behaviour and its influence on the rotor performance, as well as the numerical and experimental analysis of the effects of the wind tunnel walls on the ice accumulation on UAVs to verify the findings of this work.

Acknowledgment

The work is partly sponsored by the Research Council of Norway through the project codes 316425 IKTPLUSS and 321667 Industrial PhD. We would Jenifer Spencer and Mikko Tiihonen of the team at VTT and Henidya Hermawaran for the assistance during the experimental campaign.

References

[1] Shakhatreh, H.; Sawalmeh, A.H.; Al-Fuqaha, A.; Dou, Z.; Almaita, E.; Khalil, I.; Othman, N.S.; Khreishah, A.; Guizani, M. 486 Unmanned aerial vehicles (UAVs): A survey on civil applications and key research challenges. Ieee Access 2019

[2] Siquig, R. Impact of Icing on Unmanned Aerial Vehicle (UAV) Operations; Naval Environmental Prediction Research Facility: Monterey, CA, USA, 1990.

[3] Cao, Y.; Tan, W.; Wu, Z. Aircraft icing: An ongoing threat to aviation safety. Aerospace Science and Technology, 2018

[4] Bragg, M., Broeren, A., and Blumenthal, L., "Iced-airfoil aerodynamics," Progress in Aerospace Sciences, Vol. 41, No. 5, p. 323–362, 2005

[5] Szilder, K. and Yuan, W. In-flight icing on unmanned aerial vehicle and its aerodynamic penalties. In Proceedings of the Progress in 497 Flight Physics, Vol. 9, pp. 173–18, 2017

[6] Hann, R., Johansen, T.A. Unsettled Topics in Unmanned Aerial Vehicle Icing. SAE International, SAE EDGE Research Report EPR2020008, 2020

[7] Müller, N.C.; Hann, R., UAV Icing: A Performance Model for a UAV Propeller in Icing Conditions. In AIAA AVIATION Forum; AIAA, 2022

[8] Kozomara, D.; Neubauer, T.; Puffing, R.; Bednar, I.; Breitfuss, W. Experimental investigation on the effects of icing on multicopter UAS operation. In AIAA AVIATION FORUM 2021; AIAA, 2021

[9] Yan, S., Opazo, T., Palacios, J., Langelaan, J. W., & Germain, L. D. "Experimental evaluation of multi-rotor UAV operation under icing conditions." Annual Forum Proceedings-AHS International. Vol. 2018. American Helicopter Society, 2018

[10] Seddon, J.n M., and Simon N.. Basic helicopter aerodynamics. John Wiley & Sons, 2011

[11] Conlisk, A. T. "Modern helicopter rotor aerodynamics." Progress in aerospace sciences Volume 37, Issue 5 Pages 419-476, 2001

[12] Hann, R. & Johansen, T. A. UAV Icing: The Influence of Airspeed and Chord Length on Performance Degradation. Aircraft Engineering and Aerospace Technology 93, 832–841. ISSN: 1748-8842, 1748-8842, 2021

[13] Liu, Y., Li, L., Chen, W., Tian, W., and Hu, H., "An experimental study on the aerodynamic performance degradation of a UAS propeller model induced by ice accretion process," Experimental Thermal and Fluid Science, Vol. 102, 2019

[14] Müller, N.C.; Hann, R., UAV Icing: A Performance Model for a UAV Propeller in Icing Conditions. In AIAA AVIATION 2022 Forum; AIAA, 2022

[15] Müller, N. C., and Hann, R., "UAV Icing: 3D simulations of propeller icing effects and anti-icing heat loads" SAE Technical Paper 2023-01-1383, 2023,

[16] Tiihonen, M.; Jokela, T.; Makkonen, L.; Bluemink, G.J. VTT icing wind tunnel 2.0. In Proceedings of the Winterwind International Wind Energy Conference, 2016

[17] 1580 Test Stand Tyto Robotics. [Online]. Available: https://www.tytorobotics.com/products/series-1580-test-stand-bundle, Accessed 9.4.2024

[18] Phantom HighSpeed, VEO710L. [Online]. Available: https://phantomhighspeed.my.site.com/PhantomCommunity/s/detail/a1p3m000003lj4dAAA Accessed 9.4.2024

[19] Hann, R., Müller, N., Lindner, M., and Wallisch, J., "UAV Icing: Experimental Validation Data for Predicting ice Shapes at Low Reynolds Numbers," SAE Technical Paper 2023-01-1372, 2023

[20] SAE International, "ARP5905 Calibration and Acceptance of Icing Wind Tunnels," Aerospace Recommended Practice ARP5905, 2015

[21] Mejzlik Shop, Propeller 15x5 CCW 2B MC. [Online]. Available: thttps://shop.mejzlik.eu/propeller-15x5-ccw-2b-mc/ Accessed 9.4.2024

[22] Ghirardelli, M.; Kral, S.T.; Müller, N.C.; Hann, R.; Cheynet, E.; Reuder, J. Flow Structure around a Multicopter Drone: A Computational Fluid Dynamics Analysis for Sensor Placement Considerations. Drones 2023